# A COMPARISON OF AN IMPROVED DESIGN FOR TWO INTEGRATED OPTICAL ISOLATORS BASED ON NONRECIPROCAL MACH-ZEHNDER INTERFEROMETRY

N. Bahlmann, M. Lohmeyer, M. Wallenhorst, H. Dötsch, P. Hertel
University of Osnabrück, 49069 Osnabrück, Germany

## ABSTRACT

Nonreciprocal rib waveguide structures can be used to realize integrated optical isolators. The nonreciprocal phase shift is the difference between the forward and backward propagation constants of TM modes in magneto-optic waveguides. It can be optimized with respect to absolute value and temperature dependence if double layer waveguides with different magnetic and nonmagnetic layers are prepared. In this paper we propose an improved design for two different Mach-Zehnder interferometer isolators the nonreciprocal parts of which are formed by such double layer waveguides. One concept utilizes a nonreciprocal and a reciprocal arm. In the other case both arms are nonreciprocal but with opposite sign of the nonreciprocal phase shift. A particular property of both concepts is that the lengths of the nonreciprocal arms are well defined. The rest of the interferometer is made by reciprocal rib waveguides. Therefore, the nonreciprocal phase shift is well known. The concepts are compared with regard to isolation ratio, forward losses and fabrication tolerances. Moreover, we simulate the entire isolator by a finite difference beam propagation calculation.

## INTRODUCTION

Nonreciprocal magneto-optic devices, such as isolators or circulators, play an important role in optical technology. As they distinguish between forward and backward propagating light, they are used to protect optical components, especially lasers, from reflected light. Bulk or microoptic isolators are commercially available. Magnetic garnet films are the best choice for the realization of integrated isolators, because of their high Faraday rotation and low absorption in the near infrared.

Various kinds of optical isolators have been proposed by a number of researchers [1, 2, 3, 4, 5, 6, 7]. The most promising concepts of integrated optical isolators rely on nonreciprocal Mach-Zehnder interferometry [8, 9]. The distinction between forward and backward propagation is achieved by the differential nonreciprocal phase shift $\Delta\beta$, the difference between the forward and backward propagation constants $\Delta\beta = \beta^{\mathrm{TM}}_{\mathrm{forw}} - \beta^{\mathrm{TM}}_{\mathrm{back}}$ of TM modes in magneto-optic waveguides [10]. In forward direction, waves propagating along both arms of the Mach-Zehnder interferometer are in phase, in backward direction a phase shift of $\pi$ occurs. In this paper we present a comparison of different detailed design and fabrication considerations for the realization of such isolators. The required fabrication tolerances are estimated and beam propagation calculations are used to demonstrate how the isolators work.

## THEORY

### Nonreciprocal Waveguides

For the basic rib geometry sketched in Fig. 1 the propagation constants of TE and TM modes propagating along the $z$-axis can be calculated using a finite element [11] or a finite difference method [12]. If the magnetization $\boldsymbol{M}$ is adjusted in the film plane perpendicular to the propagation direction, a nonreciprocal phase shift $\Delta\beta$ shows up for TM modes.

Perturbation theory yields

$$\Delta\beta = \frac{\iint |H_y|^2(\partial_x \xi/\epsilon^2)dxdy}{\iint \epsilon^{-1}|H_y|^2 dxdy} \tag{1}$$

for the differential nonreciprocal phase shift [13]. $H_y$ is the field distributiuon of the unperturbed TM mode, $\epsilon$ the permittivity, and $\xi$ is related to the Faraday rotation $\Theta_{\mathrm{F}}$ by $\xi \approx 2n\Theta_{\mathrm{F}}/k_0$ where $k_0$ is the vacuum wave number.

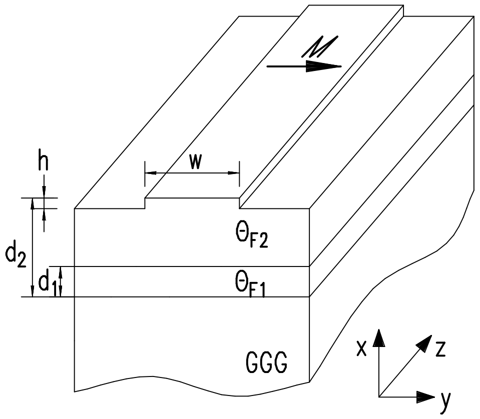


Figure 1: Basic geometry of the rib waveguide.

To achieve a large $|\Delta\beta|$, double layer garnet films with opposite Faraday rotation are prepared where the boundary between layers is located close to the maximum of $|H_y|^2$ [14]. Double layer waveguides with a positive rotating bottom layer and a negative rotating top layer show the highest differential nonreciprocal phase shift [15]. Due to the large temperature dependence of the positive Faraday-rotation such films are not suitable for the realization of a device [14]. Therefore, we use a paramagnetic bottom layer (0.18 $\mu$m thick) with negligible Faraday-rotation. The maximum nonreciprocal phase shift of 10.05 cm$^{-1}$ is achieved at a total waveguide thickness of 0.504 $\mu$m. The refractive index and the Faraday-rotation of the films are ($n$=2.2, $\Theta_{\mathrm{F}} = 0°/\mathrm{cm}$) and ($n$=2.33, $\Theta_{\mathrm{F}} = -1450°/\mathrm{cm}$), respectively.

## Nonreciprocal Mach-Zehnder Interferometer

The double layer rib waveguides described above can be used to realize the nonreciprocal part of an integrated Mach-Zehnder interferometer. Different proposals for a Mach-Zehnder type isolator have been put forward by many researchers [8, 9, 16]. Because the couplers are made by magneto-optic waveguides as well, the lengths of the nonreciprocal phase shifters are not well defined. To avoid this problem, Yokoi proposed, in ref. [17], a new design employing wafer-direct bonding.

Our concept to get rid of this problem is to replace the magnetic layer by a dielectric film for the reciprocal part. After masking the nonreciprocal waveguide sections the magnetic garnet film must be removed by ion beam etching. Afterwards this region is refilled with a dielectric layer of the same refractive index like titanium dioxide [18]. The thickness of this new layer must be well chosen in order to have equal propagation constants in the reciprocal and nonreciprocal parts. Then no reflections will occur. In this paper we propose two different isolators build with this technique. The first utilizes just one nonreciprocal interferometer arm. The rest of the Mach-Zehnder is reciprocal. For the second isolator both arms are nonreciprocal but with opposite sign of the magnetization. Therefore, the nonreciprocal effects add up (see Fig. 2).

The main advantage of the design with one nonreciprocal arm is that the whole device must be magnetized in just one direction. It is sufficient to magnetize the isolator by an

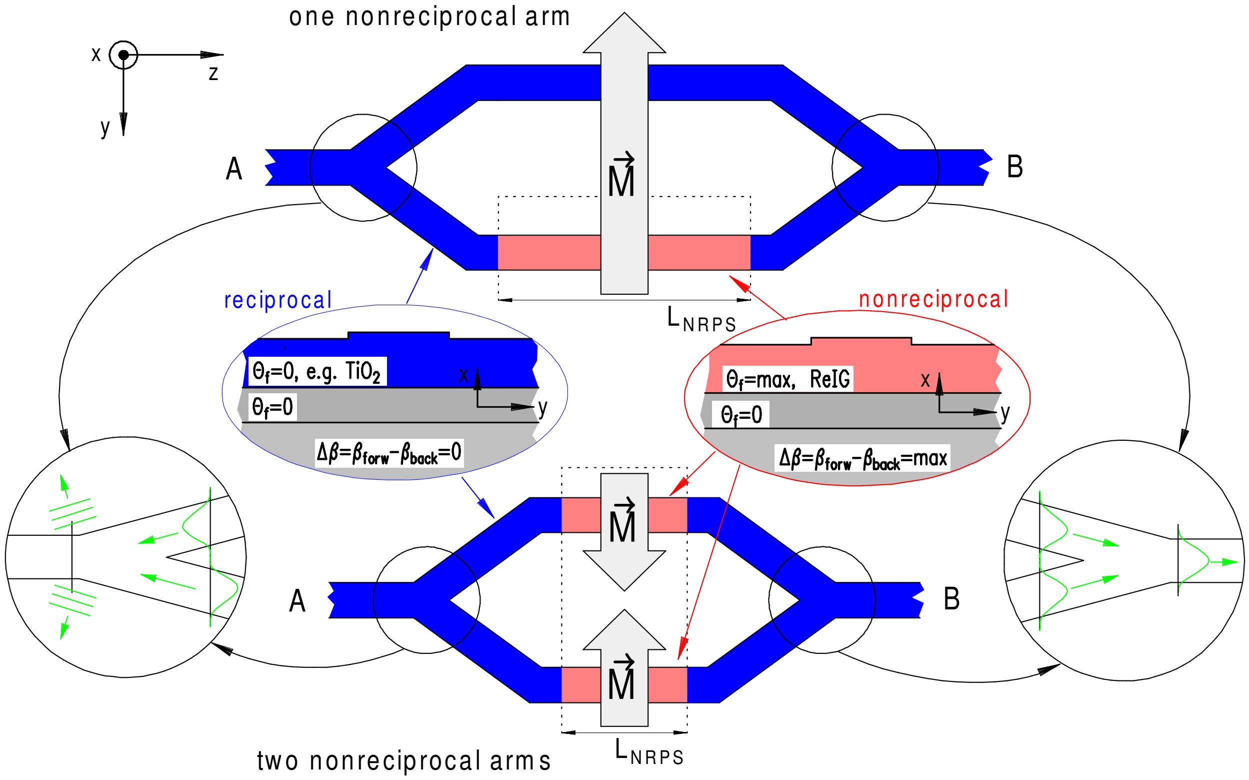


Figure 2: Basic geometry of two nonreciprocal Mach-Zehnder interferometers. The upper isolator has one nonreciprocal arm. The second one utilizes two nonreciprocal arms with opposite magnetization.

external bias magnetic field. To realize the interferometer with two nonreciprocal branches, we have to adjust the magnetization separately in each waveguide. Permanent magnets or dc electric current flowing along an electrode above the waveguides yield magnetic field opposite in the two arms. Levy et al. [2] used sputtered thin film magnets for this purpose. Thus it is possible, but it requires some additional difficult fabrication steps. The length of the well defined nonreciprocal part for the first design becomes $L_{\mathrm{NRPS}} = \pi/\Delta\beta = 0.312$ cm. This is twice as long as the reciprocal arms of the interferometer with two arms. Because of that, the losses of the device can be reduced by the second design (the losses of the y-couplers are equal in both cases). For the first design another problem occurs if the reciprocal and the nonreciprocal arms have different losses. The use of asymmetric y-splitters solves this complication but leads to unnecessary efforts.

Fabrication Tolerances

Three parameters have the strongest influence on the isolation ratio of the interferometer. The intrinsic phase difference between the arms in forward direction must vanish, whereas the total nonreciprocal phase shift in backward direction must be $\pi$. The third important factor is the splitting ratio $\bar{\alpha}$ of the y-junctions.

The intrinsic phase depends strongly on the waveguide geometry and the refractive indices. It is impossible to structure the interferometer in one step with the required accuracy. But it can be tuned in a postfabrication process by local laser annealing or stepwise reduction of the waveguide thickness in one arm. Furthermore, this is necessary to achieve an additional reciprocal phase shift of $\pi/2$ in one arm.

We estimate the isolation ratio $P_{\text{out,forw}}/P_{\text{out,back}}$ by the following expression [19]:

$$P_{\text{out}} = \frac{P_{\text{in}}}{2} K \mathrm{e}^{-\alpha L_{\text{dev}}} (1 + 2\sqrt{\bar{\alpha}(1-\bar{\alpha})} \cos\Phi). \tag{2}$$

$P_{\text{in}}$ and $P_{\text{out}}$ denote the input and output power, respectively. The damping of the waveguides is $\alpha$ and the total device length is $L_{\text{dev}}$. $K$ describes additional losses which are caused e. g. by the y-couplers. The splitting ratio of the y-couplers is described by $\bar{\alpha}$ (1/2 for ideal couplers). $\Phi$ is the phase difference between the arms. To achieve an isolation of 30 dB, the splitting ratio $\bar{\alpha}$ should range from 0.48 to 0.52 if the phase difference $\Phi_{\text{forw}} - \Phi_{\text{back}}$, which is the total nonreciprocal phase shift if $\Phi_{\text{forw}}$ is assumed to be 0, lies between 177° and 183° (see Fig. 3). This requires a thickness and length variation of the nonreciprocal waveguides smaller than $\pm 0.03$ $\mu$m and $\pm 5$ $\mu$m, respectively. For the design with two nonreciprocal arms each length must be adjusted with double precision. Otherwise the fabrication tolerances are equal in both cases, as the intrinsic phase must be tuned in a postfabrication step.

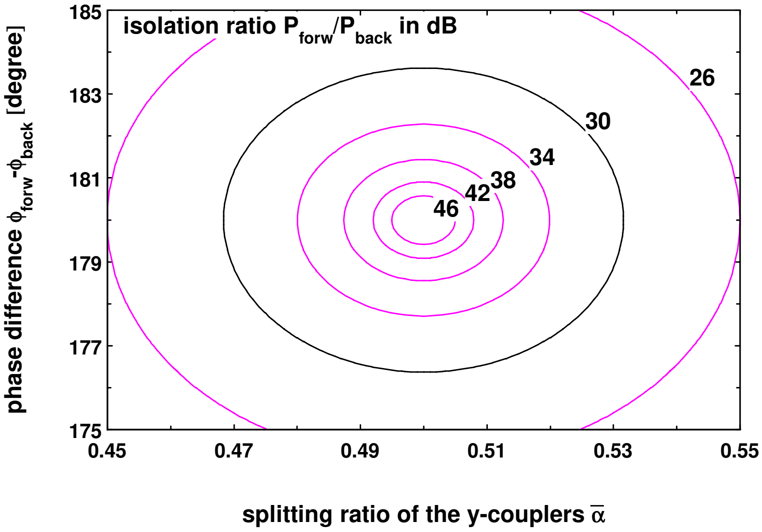


Figure 3: Calculated isolation ratio $P_{\text{forw}}/P_{\text{back}}$ for a nonreciprocal Mach-Zehnder interferometer. The intrinsic phase $\Phi_{\text{forw}}$ is assumed to be zero.

## Finite Difference Beam Propagation

In order to simulate the behaviour of nonreciprocal devices like Mach-Zehnder interferometers, we employ a finite difference beam propagation method for nonreciprocal three dimensional structures (two dimensional cross section, one propagation dimension). Different beam propagation techniques for reciprocal waveguides were introduced by a number of researchers [20]. Erdmann et. al [21] introduced a BPM method for planar magneto-optic waveguides.

The following calculations are performed with effective indices. In the magneto-optic waveguides we have different indices for forward and backward direction. Therefore, we have to carry out the BPM calculation twice. In paraxial approximation one obtains the Fresnel equation [20]

$$2\mathrm{i}k_0 n_{\text{ref}} \frac{\partial E_x}{\partial z} = \frac{\partial^2 E_x}{\partial y^2} + k_0^2 [n_{\text{eff}}^2(y) - n_{\text{ref}}^2] E_x \tag{3}$$

for the dominating electric field component $E_x$ of the TM mode. The reference index $n_{\text{ref}}$ is supplied by a calculation without magneto-optic effect. The Fresnel equation is solved with a finite difference Crank-Nicolson procedure. In order to suppress reflections from the boundaries, transparent boundary conditions are implemented [22].

Fig. 4 shows the calculated fields for the forward and backward direction. The geometry parameters of the Mach-Zehnder interferometer with one nonreciprocal arm are given in the figure caption. Almost 97 % of the input light passes the isolator in forward direction, but less than 0.1 % in backward direction, the rest leaving the device in lateral direction. This amounts to an isolation exceeding 30 dB. Calculations for the device with two nonreciprocal arms yield analogous results. Because of the space restrictions in this paper, they are not shown here.

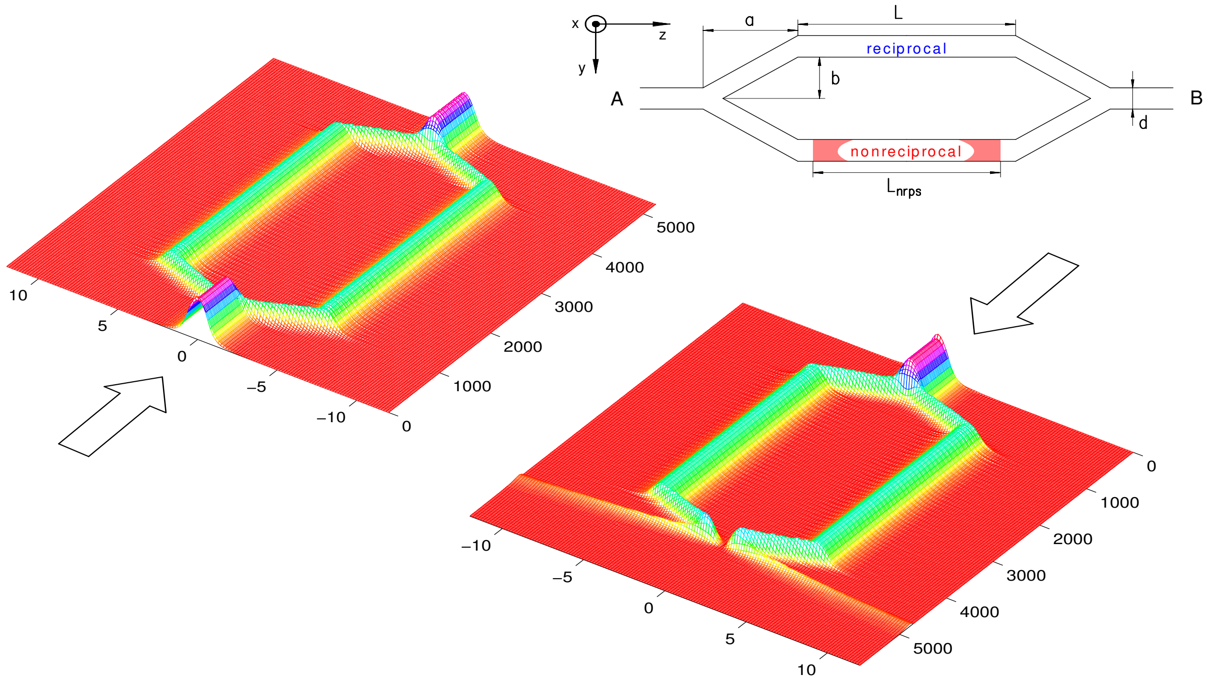


Figure 4: BPM simulation of the Mach-Zehnder interferometer. For the nonreciprocal part we use the double layer waveguide with $\Delta\beta = 10.05\ \mathrm{cm}^{-1}$. ($a = 400\ \mu\mathrm{m}$, $b = 4\ \mu\mathrm{m}$, $d = 1.5\ \mu\mathrm{m}$, $L = 3250\ \mu\mathrm{m}$, $L_{\mathrm{NRPS}} = 3123\ \mu\mathrm{m}$).

## CONCLUSIONS

Double layer rib waveguides with one paramagnetic and one magneto-optic layer are a good choice to realize nonreciprocal devices. We propose two improved designs for a nonreciprocal Mach-Zehnder interferometer isolator. An outstanding feature of the concept is that the nonreciprocal parts of the interferometers are well defined. This leads to a well known nonreciprocal phase shift. If the intrinsic phase is tuned in a postfabrication process the fabrication tolerances are almost identical for both designs. The advantage of the design with two nonreciprocal arms is the lower forward loss due to reduced length. But a reversal of the magnetization requires additional technical efforts. Therefore it seems to be wise to make first experiments with one nonreciprocal arm. Simple BPM calculations with different effective refractive indices for forward and backward direction work well to simulate the propagation of light in the device.


## ACKNOWLEDGEMENTS

We gratefully acknowledge financial support by Deutsche Forschungsgemeinschaft, Sonderforschungsbereich 225.

## REFERENCES


[1] R. Wolfe, J.F. Dillon Jr., R. A. Lieberman, and V. J. Fratello, *Applied Physics Letters*, **57**, (10), pp. 960, 1990.

[2] M. Levy, R. M. Osgood Jr., H. Hegde, F. J. Cadieu, R. Wolfe, and V. J. Fratello, *IEEE Photonics Technology Letters*, **8**, (7), pp. 903–905, 1996.

[3] K. Ando, T. Okoshi, and N. Koshizuka, *Applied Physics Letters*, **53**, (1), pp. 4–6, 1988.

[4] T. Mizumoto, Y. Kawaoka, and Y. Naito, *The Transactions of the IECE of Japan*, **E 69**, (9), pp. 968–972, 1986.

[5] H. Hemme, H. Dötsch, and P. Hertel, *Applied Optics*, **29**, (18), pp. 2741–2744, 1990.

[6] S. Yamamoto, Y. Okamura, and T. Makimoto, *IEEE Journal of Quantum Electronics*, **QE-12**, (12), pp. 764–770, 1976.

[7] T. Shintaku, *Applied Physics Letters*, **66**, (21), pp. 2789–2791, 1995.

[8] F. Auracher and H.H. Witte, *Optics Communications*, **13**, (4), pp. 435–438, 1975.

[9] Y. Okamura, T. Negami, and S. Yamamoto, *Applied Optics*, **23**, (11), pp. 1886–1889, 1984.

[10] S. Yamamoto and T. Makimoto, *Journal of Applied Optics*, **45**, (2), pp. 882–888, 1974.

[11] M. Koshiba and X.P. Zhuang, *Journal of Lightwave Technology*, **11**, (9), pp. 1453–1458, 1993.

[12] A. Erdmann, M. Shamonin, P. Hertel, and H. Dötsch, *Optics Communications*, **102**, (1,2), pp. 25–30, 1993.

[13] M. Shamonin and P. Hertel, *Applied Optics*, **33**, (27), pp. 6415–6421, 1994.

[14] M. Wallenhorst, M. Niemöller, H. Dötsch, P. Hertel, R. Gerhardt, and B. Gather, *Journal of Applied Physics*, **77**, (7), pp. 2902–2905, 1995.

[15] N. Bahlmann, V. Chandrasekhara, A. Erdmann, R. Gerhardt, P. Hertel, R. Lehmann, D. Salz, F. Schröteler, M. Wallenhorst, and H. Dötsch, *Journal of Lightwave Technology*, to be published in May 1998.

[16] T. Mizumoto, S. Mashimo, T. Ida, and Y. Naito, *IEEE Transactions on Magnetics*, **29**, (6), pp. 3417–3419, 1993.

[17] H. Yokoi and T. Mizumoto, *Electronics Letters*, **33**, (21), pp. 1787–1788, 1997.

[18] P. Löbl, M. Huppertz, and D. Mergel, *Thin Solid Films*, **251**, pp. 72–79, 1994.

[19] W. Karthe and R. Müller, *Integrierte Optik*, Akademische Verlagsgesellschaft Geest & Portig, Leipzig, 1991.

[20] Y. Chung and N. Dagli, *IEEE Journal of Quantum Electronics*, **26**, (8), pp. 1335–1339, 1990.

[21] A. Erdmann and P. Hertel, *IEEE Journal of Quantum Electronics*, **31**, (8), pp. 1510–1516, 1995.

[22] G. R. Hadley, *Optics Letters*, **16**, (9), pp. 624–626, 1991.